

Title: The current obesity “epidemic”: segregation of familial genetic risk in NHANES cohort supports a major role for large genetic effects

Running title: Segregation of familial genetic obesity risk

Authors: Arthur B. Jenkins<sup>1,4\*</sup>, Marijka Batterham<sup>2</sup>, Lesley V. Campbell<sup>3,4</sup>

<sup>1</sup> School of Medicine, University of Wollongong, Wollongong NSW 2522 Australia

<sup>2</sup> Statistical Consulting Centre, School of Mathematics and Applied Statistics, University of Wollongong NSW 2522 Australia

<sup>3</sup> Diabetes Service, St Vincent’s Hospital, Sydney, NSW 2010 Australia

<sup>4</sup> Diabetes and Metabolism Division, Garvan Institute of Medical Research, Darlinghurst, NSW 2010 Australia

\* Corresponding author

E-mail: [ajenkins@uow.edu.au](mailto:ajenkins@uow.edu.au)

The authors declare no competing financial or non-financial interests.

# Abstract

**Background/Objectives:** The continuing increase in many countries in adult body mass index (BMI kg/m<sup>2</sup>) and its dispersion is contributed to by interactions between genetic susceptibilities and an increasingly obesogenic environment. Whether population susceptibility to obesogenic environments is mainly determined by a subgroup with high genetic susceptibility or susceptibility is more evenly distributed throughout the population is unresolved, due to uncertainties around relevant genetic and environmental architecture. We aimed to test the predictions of a Mendelian genetic architecture based on collectively common but individually rare large-effect variants and its ability to account for current trends in a large population-based sample.

**Subjects/Methods:** We studied publicly available adult BMI data (n = 9102) from 3 cycles of NHANES (1999, 2005, 2013) adjusted for age, gender and race/ethnicity. A first degree family history of diabetes (FH) served as a binary marker (FH<sub>0</sub>/FH<sub>1</sub>) of genetic obesity susceptibility. We tested for multi-modality in BMI non-parametrically using a runs tests in conditional quantile regression (CQR) models of FH effects, obtained parametric fits to a Mendelian model in FH<sub>1</sub>, and estimated FH-environment interactions in CQR models and in ANCOVA models incorporating secular time.

**Results:** A unimodal FH effect on BMI was excluded (p≤0.0001) in CQR models and parametric fits to a Mendelian model in FH<sub>1</sub> identified 3 modes at 25.8±1.0 (SEM), 32.1±1.8 and 40.6±2.5 kg/m<sup>2</sup>. Mode separation accounted for ~40% of BMI variance in FH<sub>1</sub> providing a lower bound for the contribution of large effects. CQR analysis identified strong interactions between FH and environmental factors (p≤0.01) and FH<sub>1</sub> accounted for ~60% of the secular trends in BMI and its SD in ANCOVA models.

**Conclusions:** Multimodality in the FH effect is inconsistent with a predominantly polygenic small effect architecture. We conclude that large genetic effects interacting with obesogenic environment provide a better, quantitative explanation for current trends in BMI.

# Introduction

The recent and continuing increase in the global mean adult BMI, first seen in high income countries, is now apparent in most countries across a wide range of ethnic composition and socio-economic conditions (1) and is accompanied by increases in measures of dispersion (2, 3). Although BMI is known from family-based studies to be under strong genetic influences (4) population genetic backgrounds have been effectively constant over this time, implying that BMI trends are driven by change in environmental factors (obesogenic environment, OE). Evidence from twin studies, which demonstrate increased genetic variance over time, supports an important role for interactions between OE and genetic susceptibility (G x OE) on both mean and dispersion of BMI (3, 5), but how large a role is not yet clear. Defining the role of G x OE in “epidemic” obesity, and hence of genetic susceptibility itself, is hindered by problems of measurement and modeling of interactions (6) and by uncertainty around both the genetic architecture (4) and the exact nature of the environmental drivers (7). Whether a population's susceptibility to OE is predominantly determined by a subgroup with high genetic susceptibility or is more evenly spread within populations is unresolved despite important implications for the management of obesity and related disorders at population and individual levels (2, 8–10).

The genetic variants responsible for obesity susceptibility remain largely unknown. Genome-wide association studies (GWAS) have identified significant associations with >200 markers with small effects on BMI (polygenes), together explaining only approximately 3-4 % of total variance compared to family-based heritabilities ( $h^2$ ) of 50-75% (11). Few causative mechanisms responsible for these phenotypically weak associations are known (4). The sources of the  $h^2$  unaccounted for by GWAS are uncertain; proposals include overestimation of  $h^2$ , large numbers of common genetic variants with small, statistically insignificant effects on phenotypes (12, 13) and importantly, candidates not tested in most GWAS. Among the latter are rare genetic variants with large phenotypic

effects and G x OE interactions (4). Recently significant G x OE interactions have been detected in individual GWAS loci and in composite genetic risk scores, which explain little of the missing component of  $h^2$  (14, 15).

A family history of diabetes (FH) is a potent, predominantly genetic (16, 17) risk factor for diabetes diagnosis (DM) and for obesity-related phenotypes (18–21) consistent with the strong association between type 2 DM and overweight/obesity. Familial effects on obesity-related phenotypes in adults are also predominantly genetic (3, 22), so to the extent that the DM generating FH is of type 2 (approximately 94% of DM in the US population (23)), FH is a prevalent and readily obtained marker of genetic susceptibility both to diabetes and to the obesity commonly preceding it. We have reported evidence from a small sample of a multi-modal effect of FH on a composite adiposity index consistent with segregation in families of discrete obesity risk (21). Polygenic risk scores (PRS) based on large numbers of small effects are expected to be, and appear to be, normally-distributed (24, 25) and cannot account for familial segregation of risk. The present work is based on the alternative hypothesis that individually rare, but collectively common, genetic variants with large phenotypic effects are the source of most of the missing  $h^2$  and of most of G x OE, and that their effects can be detected through analyses of phenotypic segregation in high-risk families (26).

The Continuous National Health and Nutrition Examination Survey (NHANES) is a continuing (1999-) large-scale population-based survey incorporating an index of adiposity (Body Mass Index, BMI) and first-degree FH (FH<sub>0</sub>/FH<sub>1</sub>) together with potential covariates and confounders. Although BMI has recognized limitations as an adiposity phenotype (26, 27) it is the basis for most large-scale genetic studies and like other authors, we assume that a large enough scale and appropriate modeling of covariates will reduce effects of imprecision and bias (11). We aimed to test in a large multi-cycle NHANES sample for the presence of familial segregation of genetic risk and to estimate the contribution of FH, and by extension all discrete genetic risk, to recent secular trends in adult BMI.



Our results support a predominant role for large genetic effects interacting with OE in the obesity “epidemic”.

## Data and Methods

### Data

We used data from the 1999-2000, 2005-2006 and 2013-2014 cycles of NHANES (<https://www.cdc.gov/nchs/nhanes/index.htm> accessed 25 Aug 2017). We extracted records for participants age 20-65 years with non-missing gender, race/ethnicity, BMI, diabetes family history (FH) and diabetes diagnosis data, and current smoking status if available. The definitions of two fields changed over the sampling period: 1) Diabetes family history was defined in terms of 1° and 2° relatives in 1999-2000 but by 1° relatives only in subsequent cycles. We recoded the 1999-2000 diabetes family history data to conform to the later definition using the separately collected data for affected parents and siblings. 2) The self-identified race/ethnicity field (RIDRETH1) code was used excluding other races (OR) to maintain consistency across cycles (Supplementary Methods). We excluded from the primary analyses subjects diagnosed with diabetes because of possible confounding by effects of either diabetes or diabetes therapies on BMI. The resulting data set is summarized in Table 1.

### Statistical analyses

#### *Approach*

We treat the data as a convenience sample and took no account of the sampling weights provided by NHANES to permit nationally representative estimates. Our results are not intended to be representative of the US population.

Our primary analyses are based on non-parametric visualization (kernel-smoothing) and analyses (conditional quantile regression, CQR) of distributions requiring no prior distributional assumptions. Parametric fits to multimodal distributions were then used to quantify the contributions of the predicted large genetic effects model. FH(0/1) is treated as a binary genetic risk marker and calendar time as a continuous surrogate of OE. Effects of OE interacting with FH were assessed in CQR models, and also in least-squares ANCOVA models using bootstrap resampling to minimize distributional assumptions in the calculation of effect size estimates and errors. All analyses were performed using R 3.3.1 (28).

#### *Summary statistics*

Heterogeneity of the samples across cycles was assessed by Chi square test for categorical variables and by one-way ANOVA for age. Effects on BMI were assessed by ANCOVA against continuous time (yr = calendar start year - 1999). Effects on phenotype SD's were assessed by Bartlett's test in one-way ANOVA models.

#### *Adjustment*

Prior to analysis BMI was adjusted for effects of age, gender and race/ethnicity in a linear model (age + age<sup>2</sup> + race x gender). The adjustment model accounted for 4 % of the total variance in BMI (Supplementary Table S1).

## Distributions

### Visualization

The effect of FH on the distribution of adjusted BMI was visualized using kernel-smoothed density estimates by FH status (R base function `density`). The degree of smoothing is controlled by the bandwidth parameter (`bw`) which was obtained in the full non-diabetic data set ( $bw = 0.99$ ) from a measure of the dispersion of the data (29). This produces a continuous distribution function and is widely used to visualise features of potential interest which may be obscured in histograms. The credibility of apparent effects of FH on the shape of the distribution was assessed by post-hoc analysis of density differences ( $FH_1 - FH_0$ ) by quantiles ( $n=20$ ) of the full sample. Mean density differences with SE were obtained by quantile by bootstrap resampling with replacement (1000 draws, stratified by FH status with resample sizes = strata sizes) and tested against zero using a Z-test.

### Conditional Quantile Regression (CQR)

Conditional quantile regression is a powerful tool for analyzing the effect of covariates on distributions without assumptions of distributional shape. In contrast to ordinary least-squares (OLS) regression which characterizes effects on global features of a distribution, CQR analyses local effects of covariates independently at any specified quantiles and can detect and test variations in covariate effects across quantiles. Originating in econometrics (30) it is now used in other areas including genetics (31). In the CQR framework developed by Abadi et al (14) for analysis of genomic markers, trends in effect sizes across quantiles represent interactions between genetic effects and unobserved environmental and/or genetic factors. We treat FH as a binary genetic risk marker ( $FH_0/FH_1$ ) and a linear trend in quantile regression coefficients ( $\beta_{1i}$ ) across quantiles ( $\tau_i$ ) represents summed linear interactions of FH with unobserved factors. We analysed the effects of FH on adjusted BMI by CQR

using the R package quantreg. The effect of all interactions on the FH effect was tested in a 2 parameter linear model:

for each quantile  $\tau_i$  in  $y$ ,

$$y(\tau_i | FH=fh) = \beta_{0i} + \beta_{1i} * FH$$

where  $y(\tau_i | FH=fh)$  = the  $i$ th quantile of adjusted BMI conditional on the value of FH (0,1), the intercept  $\beta_{0i}$  is the  $i$ th quantile value in  $FH_0$  and  $\beta_{1i}$  is the FH effect size in quantile  $i$ .

The interaction between FH and continuous calendar time was estimated in the ANCOVA model:

$$y(\tau_i | FH=fh) = \beta_{0i} + \beta_{1i} * FH + \beta_{2i} * yr + \beta_{3i} * FH * yr$$

where  $yr$  = cycle start year – 1999,  $\beta_{0i}$  is the  $i$ th quantile value in  $FH_0$  at  $yr = 0$  and  $\beta_{2i}$  and  $\beta_{3i}$  are CQR coefficients for time and time\*FH interaction effects in quantile  $i$ .

Equality of CQR parameter effect sizes across quantiles was tested using a Khmaladze test (32) (R package quantreg).

The shape of the interaction relationship on the BMI scale was assessed in an OLS relationship between quantile coefficients  $\beta_1$  and  $\beta_0$ , which represents a linear model of a transformed quantile-quantile plot between  $FH_1$  and  $FH_0$  after adjustment for covariates, and models a unimodal effect. Residuals from the relationship were tested against randomness using a Wald-Wolfowitz runs test (R package randtests), a simple, general non-parametric test of randomness in ordered binary observations. The number of runs is compared to expectations under a normal approximation to the random sampling distribution. Randomness is rejected in a two-sided test if the number of observed runs is too high indicating high frequency oscillations, or too low indicating longer structures. We applied a left-sided runs test to residuals from regression relationships testing for large structures and

interpret significance as excluding a unimodal effect and therefore as evidence of multiple modes in the effect.

# Parametric fits

We obtained fits to a 3-component normal mixture distribution representing a simple Mendelian model of fixed genetic effect using an expectation-maximization algorithm (normalmixEM function in the R package mixtools) . The models are characterised by the fitted means ( $\mu_i$ ), standard deviations ( $\sigma_i$ ) and mixing proportions ( $\lambda_i$ ) of the three component distributions. Full model fits were obtained in FH<sub>1</sub> but were not obtainable in FH<sub>0</sub> or DM<sub>1</sub> groups and we constrained  $\mu_i$  in those groups to values estimated in FH<sub>1</sub> in order to obtain comparable estimates of  $\sigma_i$  and  $\lambda_i$ . Risk allele frequencies (q) under an additive Mendelian model of large genetic effects were calculated from the fitted  $\lambda_i$ :

$$q = 0.5*\lambda_2 + \lambda_3$$

where  $\lambda_2$  and  $\lambda_3$  represent the proportions of carriers of 1 and 2 risk alleles respectively. Within-sample consistency of calculated q across the three groups analysed was assessed by comparing fitted  $q_{FH_1}$  with the prediction from random mating of DM<sub>1</sub> into the full sample:

$$\text{predicted } q_{FH_1} = (q_{DM} + n\text{-weighted mean}(q_{DM}, q_{FH_1}, q_{FH_0}))/2$$

# Secular trends

Effects of diabetes family history status (FH<sub>0</sub>, FH<sub>1</sub>) and continuous time (yr = calendar start year - 1999) on adjusted BMI and its standard deviation (SD) were assessed in ANCOVA models of the form:

$$y = \beta_0 + \beta_1 * FH + \beta_2 * yr + \beta_3 * FH * yr$$

where  $y$  = adjusted BMI mean or SD by FH status (0/1) and cycle, and  $yr$  = cycle start year – 1999. Each OLS fit estimated 4 parameters from the 6 data points. Mean parameter estimates with 95% CI were obtained by bootstrap resampling with replacement (1000 draws stratified by FH status and cycle with resample sizes = strata sizes).

# *Comparison of cross-sectional and secular trend effects*

Effects of FH on BMI distribution and on secular trends in BMI were compared by calculating the contribution (%) of  $FH_1$  to the effect in the full non-diabetic sample for calculated risk allele frequency ( $q\%$ ) and to the slope ( $\beta\%$ ) of the relationships between time and BMI in ANCOVA model described above. Mean ( $\pm$  SE where possible)  $q\%$  and  $\beta\%$  were calculated in the relevant bootstrap samples.

## Results

### **Participant characteristics**

Data from 9102 non-diabetic subjects met the inclusion criteria, approximately equally distributed across the 3 cycles. Gender balance varied little but there was a cycle effect in race/ethnicity, most obvious in the reduced representation of MA in the two later cycles. Average age varied across cycles but not its SD, while adjusted BMI and its SD showed linear trends with cycle time.  $FH_1$  prevalence was higher in the two later cycles compared to 1999-2000 as was  $DM_1$  prevalence. Current smoking status was predominantly missing in the data (55%) and was not included in the BMI adjustment model. However smoking status was not related to FH whether analysed in the full data ( $X^2 = 2.80$ , 2 df,  $p = 0.25$ ) or in those with non-missing smoking status ( $X^2 = 0.43$ , 1 df,  $p = 0.51$ ), hence is

unlikely to confound analyses of FH effects. The mean age at diagnosis of DM (43.6 yr) is consistent with predominantly type 2 DM in the sample.

## Distributions

### Visualization

Adjusted BMI in the non-diabetic sample showed an apparently unimodal distribution, right-skewed compared to a normal model and closer to a log-normal model (Fig 1A). When visualized by FH status (Fig 1B) the predicted multimodality in FH<sub>1</sub> was indicated with modes in the normal weight, overweight and obese regions of the BMI distribution. In contrast FH<sub>0</sub> showed an apparently unimodal distribution and a difference in shape between the two groups was supported by the pattern of formal significance in the post-hoc analysis of density differences between groups (Fig 1B). BMI distribution in the diabetic sample appeared to be depleted in the lower mode and enriched in the upper modes compared to FH<sub>1</sub> (Fig 1C).

### CQR

Analysis of the effect of FH status on the shape of the BMI distribution using CQR demonstrated increasing FH effect size at higher levels of BMI ( $p \leq 0.01$ , Fig 2A, main panel), indicating strong interactions between FH<sub>1</sub> and other variables not included in the model. FH<sub>1</sub> effect size ranged from  $< 1 \text{ kg/m}^2$  in the lower quantiles to  $\sim 3 \text{ kg/m}^2$  in the upper quantiles, substantially different in both regions to the OLS estimate ( $1.7 \text{ kg/m}^2$ ). The approximate linearity of FH<sub>1</sub> effects by quantile seen in main panel of Fig 2A supports simple 1<sup>st</sup> order interactions, with that linearity emphasised by an OLS analysis on the BMI scale between quantile coefficients  $\beta_1$  (FH<sub>1</sub>) and  $\beta_0$  (FH<sub>0</sub>) (slope =  $0.148 \pm 0.003$  (SE),  $R^2 = 0.98$ ). Adjustment for main and interaction effects of calendar time in the model (Supplementary Fig S2) weakened the trend in  $\beta_1$  across quantiles ( $p > 0.1$ , Fig 2B main panel) and the OLS relationship between  $\beta_1$  and  $\beta_0$  (slope =  $0.103 \pm 0.006$ ,  $R^2 = 0.86$ ), supporting the conclusion

that calendar time is a strong surrogate of obesogenic environmental influences interacting with genetic factors as represented by FH status.

While the overall OLS relationship between  $\beta_1$  and  $\beta_0$  was linear there was strong evidence for additional non-linear structure in an analysis of residuals from the relationship (Fig 2A inset) which found significant non-randomness (runs test,  $p = 7.4 \times 10^{-5}$ ) attributable to a small number of broad excursions. Adjustment for time effects accentuated the pattern (Fig 2B inset, runs test  $p = 2.2 \times 10^{-5}$ ).

While these patterns in the conditional quantiles do not map directly onto the unconditional quantile plots in Fig 1B, by rejecting the unimodal effect hypothesis they add strong support to the conclusion that FH<sub>1</sub> has multimodal discrete effects on BMI. The pattern of residuals after adjustment for time effects (Fig 2B inset) exhibits 3 broad peaks, with suggestions of finer structure particularly in the central peak. The lower peak in the low-normal weight range may derive from the presence of type 1 diabetes family history in the sample, while the upper two are consistent with the predicted discrete effects of FH<sub>1</sub> derived from type 2 diabetes.

# Parametric analysis

The distribution of BMI in FH<sub>1</sub> appears consistent with a simple Mendelian model and fitting a 3-component normal distribution model to the FH<sub>1</sub> data resulted in robust estimates of component means and separations (Fig 3A), as well as mixing coefficients and SDs (Table 2). Approximately 50% of FH<sub>1</sub> occupied the upper two modes and separation between modes accounted for approximately 40% of the total variance in adjusted BMI with the remainder assigned to dispersion within modes (Fig 2B). Under a Mendelian model the variance due to mode separation represents a lower bound on the contribution of large effects as some of the dispersion within modes represents variance in effect sizes of individual contributing causal loci (see Discussion) which will contribute to the ~60% of variance assigned to within-modes. Estimates of component SDs and mixing proportions with component means, constrained for FH<sub>0</sub> and DM<sub>1</sub> to those identified in the FH<sub>1</sub> data, support enrichment in the two upper components in FH<sub>1</sub> compared to FH<sub>0</sub> (48% vs. 33%) and more strongly



in DM<sub>1</sub> (72%). Predicted risk allele frequencies in FH<sub>1</sub> (q - Table 2) express these distributional properties in Mendelian terms and show within-sample consistency in that q<sub>FH1</sub> predicted from random mating of DM<sub>1</sub> (0.37) is not different to the fitted estimate (0.30 ± 10).

## Secular trends

Adjusted BMI mean (Fig 2A) and SD (Fig 2B) increased over the sampling period significantly faster in FH<sub>1</sub> compared to FH<sub>0</sub> in the bootstrapped ANCOVA model, and estimates of  $\beta$  and  $\Delta\beta$  in the mean data were indistinguishable from the OLS estimates provided by the CQR analysis (Supplementary Fig S2). Similar results were obtained with log-transformed BMI (Supplementary Fig S3). FH<sub>1</sub> accounted for 62% of the BMI mean trend and 60% of the BMI SD trend in this sample over the period 1999-2014, effects similar in magnitude to the estimated FH<sub>1</sub> contribution to the sample risk allele frequency (50%, Supplementary Table S2).

## Discussion

### Summary

We tested the prediction of segregation of discrete effects of FH on adult BMI (21), modeled as modes of distribution, and estimated the contribution of FH<sub>1</sub> to recent trends in BMI mean and dispersion in a large population-based sample. The results support a predominant role in the recent obesity "epidemic" for rare genetic variants with large effects interacting with OE.

### Segregation of genetic susceptibility

The non-parametric analysis provided evidence for a multi-modal distribution in the FH<sub>1</sub> group consistent with the prediction of segregation of large genetic effects in families (21). Multi-modality was supported by the analysis of density differences between FH<sub>1</sub> and FH<sub>0</sub> by unconditional quantiles

(Fig 1B) and by evidence of shape in the relationship between CQR coefficients on the BMI scale (Fig 2A&B insets). Polygenic risk scores (PRS) in population-based samples are expected to be normally-distributed, and appear to be so (24, 25). Any elevated polygenic obesity risk in  $DM_1$  will dilute into the mating population resulting in a right-shifted distribution in  $FH_1$  compared to  $FH_0$ , not multi-modality. Alternative explanations for multi-modality might be discrete stratification of OE which seems unlikely, or un-modeled interactions between FH and other covariates. Un-modeled interactions between FH and stratified residual confounders may exist and contribute but we found no evidence for this in plots of distributions by gender and race/ethnicity (Supplementary Fig S1) or in an analysis of smoking status against FH. Discrete inheritance of genetic variants with large effects remains the most likely explanation for multi-modality in the BMI distribution.

Approximately 40% of the adjusted BMI variance in  $FH_1$  was accounted for by between-modes variance (Fig 3B) but this represents a lower bound since the identified modes are likely to be synthetic ie composed of a range of effect sizes due to rare variants at different loci. Indications of fine structure within the broad peaks (Fig 2B inset) are suggestive. Examples of rare variants with large effects on BMI in adults ( $\beta$ ) are known from studies of candidate genes and monogenic obesity loci (26) while more recently a common variant in Samoans ( $EAF = 0.26$ ,  $\beta \approx 1.4 \text{ kg/m}^2$ ), very rare in other populations (33), and an African-specific rare variant ( $EAF = 0.008$ ,  $\beta = 4.6 \text{ kg/m}^2$ ) undetected in Europeans and Asians (34) have been identified by GWAS. Overall,  $\beta$  in these nine examples ranges from 1.4- 9  $\text{kg/m}^2$  and a similar range in effect sizes in the NHANES sample would contribute substantially to the within-mode variance estimated here. A combination of within-subject variance ( $\sim 5\%$  (35)) with polygenic variance ( $\sim 5\%$  (4)) sets a lower bound for within-modes variance and hence the upper bound for between modes, implying that between 40% and 90% of total variance in  $FH_1$  may be attributed to large genetic effects.

## G x OE

FH<sub>1</sub> is a prevalent (36%) and powerful determinant of the rate of change of mean BMI and its dispersion over time, accounting for 62% of the BMI trend and 60% of the BMI SD trend in this sample over 1999-2014. Under a polygenic model the familial risk would be distributed normally over FH<sub>1</sub> which would then be a marker of a large fraction of the at-risk population. However under the Mendelian model supported here genetic risk would segregate in families and only approximately 50% of FH<sub>1</sub> would acquire the excess familial risk and only ~18% of the sample would then account for ~60% of the trends. Individuals with DM<sub>1</sub> must represent a fraction of individuals with elevated genetic obesity risk and it is likely that the remainder, particularly those with a family history of obesity without DM, would substantially increase the genetic component of the trends consequent to the high heritability of BMI (22). This Mendelian model is internally consistent in estimates of risk allele frequencies (q) in FH<sub>1</sub>, FH<sub>0</sub> and DM<sub>1</sub> (Table 2) and in comparisons of FH<sub>1</sub> effect sizes in cross section (q, ~50%) and over time (β, ~60%) (Supplementary Table S2). Our results support the proposition that the largest part and perhaps all of recent trends in mean and dispersion of BMI are due to a minor subset of individuals with elevated genetic susceptibility to OE.

## Limitations

The design and interpretation of fits to parametric mixture distribution models involves choices concerning the number of components, parameter starting values and algorithms, and fit to a specific model cannot be taken in isolation as support for its structural validity. We base our choice and structural interpretation of 3-component normal mixture model fits and parameters on the *a priori* hypothesis of Mendelian segregation of obesity risk in families (21) supported by the non-parametric distributional plots (Fig 1B,C) and CQR analysis (Fig 2A,B insets). Like Abadi et al (14) we interpret interactions in the CQR analysis as predominantly G x OE although a contribution from G x G interactions cannot be excluded. Our interpretation is supported by the effects on the interaction of

including calendar time in the CQR model (Fig 2B). Other limitations discussed above include our inability to exclude discrete stratification of OE and the possible influence of unmeasured/unknown confounders of FH.

## Conclusions

We conclude that a Mendelian model of individually rare but collectively common genetic risk variants with large effects interacting with OE provides a plausible quantitative explanation for recent trends in obesity and should be favored over a predominantly polygenic model which does not. The evidence for a predominant role for polygenes (13) can appear to be strong (eg “Polygenic obesity is the most common form of obesity in modern societies...” (36)) but recent interpretations seek to explain the still missing heritability in obesity in terms of unidentified large genetic effects and G x OE (4, 37) and recommend a renewed focus on family-based designs and on specific populations in which large effect variants may be enriched (33, 34). Our results strengthen that view by showing that a model based on unidentified segregating variants with large effects interacting with OE can account for the largest part of the secular trend in obesity and its dispersion in a large population-based sample. We can’t predict what positive clinical or public health changes might follow from these findings but they should help refocus research away from the under-performing but entrenched big idea (38) that is polygenic obesity.

Supplementary information is available at The International Journal of Obesity’s website.

**Supplementary Methods:** Race/Ethnicity coding

**Supplementary Table S1:** BMI-adjustment model parameters

**Supplementary Table S2:** Comparison of effects of diabetes family history on secular trends in adjusted BMI and its SD and on calculated risk allele frequencies (q) in non-diabetic participants.

**Supplementary Fig S1:** Kernel-smoothed adjusted BMI densities by FH, gender and race/ethnicity

375 **Supplementary Fig S2:** time and time x FH interaction effects in a Conditional quantile regression  
 376 of adjusted BMI in an ANCOVA model.

377 **Supplementary Fig S3:** Secular trends in log-transformed adjusted BMI mean and SD

378

## 379 Competing Interests

380 The authors declare no competing financial or non-financial interests.

381

382

## 383 References

- 384 1. Di Cesare M, Bentham J, Stevens GAA et al. Trends in adult body-mass index in 200 countries  
385 from 1975 to 2014: a pooled analysis of 1698 population-based measurement studies with 19.2  
386 million participants. *Lancet*. 2016;387:1377-1396.
- 387 2. Krishna A, Razak F, Lebel A, Davey Smith G, Subramanian SV. Trends in group inequalities  
388 and interindividual inequalities in BMI in the United States, 1993–2012. *Am J Clin Nutr*.  
389 2015;101:598-605.
- 390 3. Silventoinen K, Jelenkovic A, Sund R et al. Differences in genetic and environmental variation  
391 in adult BMI by sex, age, time period, and region: an individual-based pooled analysis of 40  
392 twin cohorts. *Am J Clin Nutr*. 2017;106:457-466.
- 393 4. Loos RJ. The genetics of adiposity. *Curr Opin Genet Dev*. 2018;50:86-95.
- 394 5. Rokholm B, Silventoinen K, Ångquist L, Skytthe A, Kyvik KO, Sørensen TI. Increased genetic  
395 variance of BMI with a higher prevalence of obesity. *PLoS One*. 2011;6:e20816.
- 396 6. Franks PW, McCarthy MI. Exposing the exposures responsible for type 2 diabetes and obesity.  
397 *Science*. 2016;354:69-73.
- 398 7. Hall KD. Did the Food Environment Cause the Obesity Epidemic? *Obesity*. 2018;26:11-13.
- 399 8. Kivimaki M, Stenholm S, Kawachi I. The widening BMI distribution in the United  
400 States[letter]. *Am J Clin Nutr* 2015;101(6):1307-1308.
- 401 9. Jenkins AB, Campbell LV. Variation in Genetic Susceptibility Drives Increasing Dispersion of  
402 Population BMI[letter]. *Am J Clin Nutr* 2015;101:1308.
- 403 10. Razak F, Smith GD, Krishna A, Lebel A, Subramanian SV. Variation in genetic susceptibility  
404 drives increasing dispersion of population BMI Reply[letter]. *Am J Clin Nutr*  
405 2015;101(6):1308-1309.

11. Speakman JR, Loos RJF, O’Rahilly S, Hirschhorn JN, Allison DB. GWAS for BMI: a treasure trove of fundamental insights into the genetic basis of obesity. *Int J Obes.* 2018;42:1524-1531.
12. Locke AE, Kahali B, Berndt SI et al. Genetic studies of body mass index yield new insights for obesity biology. *Nature.* 2015;518:197-206.
13. Khera AV, Chaffin M, Wade KH et al. Polygenic Prediction of Weight and Obesity Trajectories from Birth to Adulthood. *Cell.* 2019;177:587-596.e9.
14. Abadi A, Alyass A, Robiou du Pont S et al. Penetrance of Polygenic Obesity Susceptibility Loci across the Body Mass Index Distribution. *Am J Hum Gen.* 2017;101:925-938.
15. Nagpal S, Gibson G, Marigorta U. Pervasive Modulation of Obesity Risk by the Environment and Genomic Background. *Genes.* 2018;9:doi: 10.3390/genes9080411.
16. Hemminki K, Li X, Sundquist K, Sundquist J. Familial risks for type 2 diabetes in Sweden. *Diabetes Care.* 2010;33:293-297.
17. Willemsen G, Ward KJ, Bell CG et al. The Concordance and Heritability of Type 2 Diabetes in 34,166 Twin Pairs From International Twin Registers: The Discordant Twin (DISCOTWIN) Consortium. *Twin Res Hum Genet.* 2015;18:762-771.
18. Ghosh A, Liu T, Khoury MJ, Valdez R. Family History of Diabetes and Prevalence of the Metabolic Syndrome in U.S. Adults without Diabetes: 6-Year Results from the National Health and Nutrition Examination Survey (1999-2004). *Public Health Genom.* 2010;13:353-359.
19. Tirosh A, Shai I, Afek A et al. Adolescent BMI trajectory and risk of diabetes versus coronary disease. *N Engl J Med.* 2011;364:1315-1325.
20. Scott RA, Consortium I. The link between family history and risk of type 2 diabetes is not explained by anthropometric, lifestyle or genetic risk factors: the EPIC-InterAct study. *Diabetologia.* 2013;56:60-69.
21. Jenkins AB, Batterham M, Samocha-Bonet D, Tonks K, Greenfield JR, Campbell LV. Segregation of a latent high adiposity phenotype in families with a history of type 2 diabetes

mellitus implicates rare obesity-susceptibility genetic variants with large effects in diabetes-related obesity. PLoS One. 2013;8:e70435.

22. Stryjecki C, Alyass A, Meyre D. Ethnic and population differences in the genetic predisposition to human obesity. Obes Rev. 2018;19:62-80.

23. Xu G, Liu B, Sun Y et al. Prevalence of diagnosed type 1 and type 2 diabetes among US adults in 2016 and 2017: population based study. BMJ. 2018;362:k1497.

24. Llewellyn CH, Trzaskowski M, Plomin R, Wardle J. From modeling to measurement: developmental trends in genetic influence on adiposity in childhood. Obesity. 2014;22:1756-1761.

25. Rask-Andersen M, Karlsson T, Ek WE, Johansson A. Gene-environment interaction study for BMI reveals interactions between genetic factors and physical activity, alcohol consumption and socioeconomic status. PLoS Genet. 2017;13:e1006977.

26. Jenkins AB, Campbell LV. Future management of human obesity: understanding the meaning of genetic susceptibility. Adv Genomics Genet. 2014;4:219-232.

27. Müller MJ, Geisler C, Blundell J et al. The case of GWAS of obesity: does body weight control play by the rules. Int J Obes. 2018

28. R Development Core Team. R: A Language and Environment for Statistical Computing. R Foundation for Statistical Computing, Vienna, Austria. URL <https://www.R-project.org/>; 2016.

29. Sheather SJ, Jones MC. A Reliable Data-Based Bandwidth Selection Method for Kernel Density Estimation. J Roy Stat Soc B Met. 1991;53:683-690.

30. Koenker R. Quantile Regression: 40 Years On. Ann Rev of Econ. 2017;9:155-176.

31. Briollais L, Durrieu G. Application of quantile regression to recent genetic and -omic studies. Hum Genet. 2014;133:951-966.

32. Koenker R, Xiao Z. Inference on the quantile regression process. Econometrica. 2002;70:1583-1612.



33. Minster RL, Hawley NL, Su CT et al. A thrifty variant in CREBRF strongly influences body mass index in Samoans. *Nat Genet.* 2016;48:1049-1054.
34. Chen G, Doumatey AP, Zhou J et al. Genome-wide analysis identifies an African-specific variant in SEMA4D associated with body mass index. *Obesity.* 2017;25:794-800.
35. Wormser D, White IR, Thompson SG, Wood AM. Within-person variability in calculated risk factors: Comparing the aetiological association of adiposity ratios with risk of coronary heart disease. *Int J Epidemiol.* 2013;42:849-859.
36. Albuquerque D, Nóbrega C, Manco L, Padez C. The contribution of genetics and environment to obesity. *Br Med Bull.* 2017;123:159-173.
37. Saeed S, Arslan M, Froguel P. Genetics of Obesity in Consanguineous Populations: Toward Precision Medicine and the Discovery of Novel Obesity Genes: Obesity and Consanguinity. *Obesity.* 2018;26:474-484.
38. Joyner MJ, Paneth N, Ioannidis JP. What Happens When Underperforming Big Ideas in Research Become Entrenched? *JAMA.* 2016;316:1355-1356.

# Figure legends

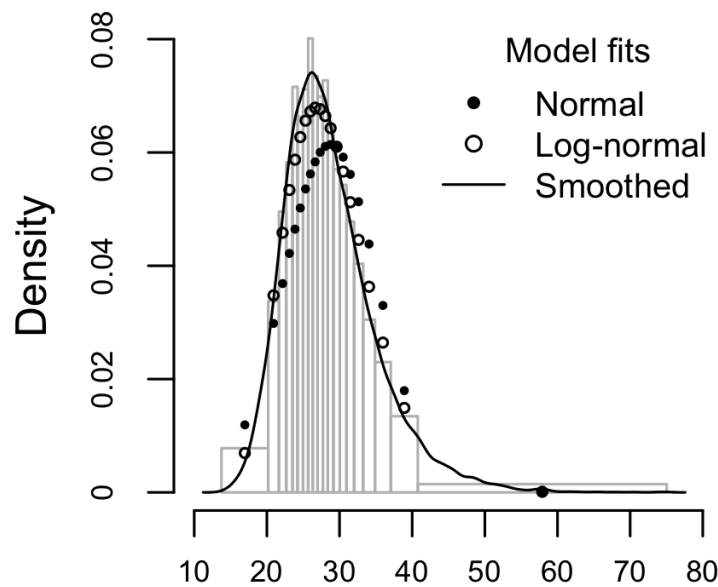
**Fig 1:** Distribution of adjusted BMI in non-diabetic ( $DM_0$ ) and diabetic ( $DM_1$ ) participants in combined NHANES 1999-2000, 2005-2006 and 2013-2014 cycles. A) Full non-diabetic sample ( $n=9102$ ) binned by quantiles ( $n=20$ ) with superimposed kernel-smoothed and fitted densities in normal and log-normal models. B) Kernel-smoothed adjusted BMI density by FH status. \* significant ( $p<0.05$ ) difference in empirical density ( $FH_1 - FH_0$ ) by quantiles of the full sample shown in panel A. C) Kernel -smoothed adjusted BMI density in non-diabetic  $FH_1$  ( $n=3297$ ) compared to diabetic participants ( $n=793$ ).

**Fig 2:** Conditional quantile regression effects of FH on adjusted BMI in non-diabetic participants in models consisting of FH alone (A) and in interaction with calendar time (B). The main panels show the FH main effect size ( $\beta_1$ ) by quantile with 95% CI (grey-shaded area), the OLS estimate of the average effect (solid black line) with 95% CI (dotted black lines) and p-values associated with Khmaladze tests for equality of  $\beta_1$  across quantiles. The insets show the patterns of residuals ( $\Delta\beta_1$ ) from linear regressions of  $\beta_1$  against conditional quantiles in  $FH_0$  ( $\beta_0$ ), with 95% CI on the fits (dotted lines) around the lines  $\Delta\beta_1 = 0$  representing perfect fits.

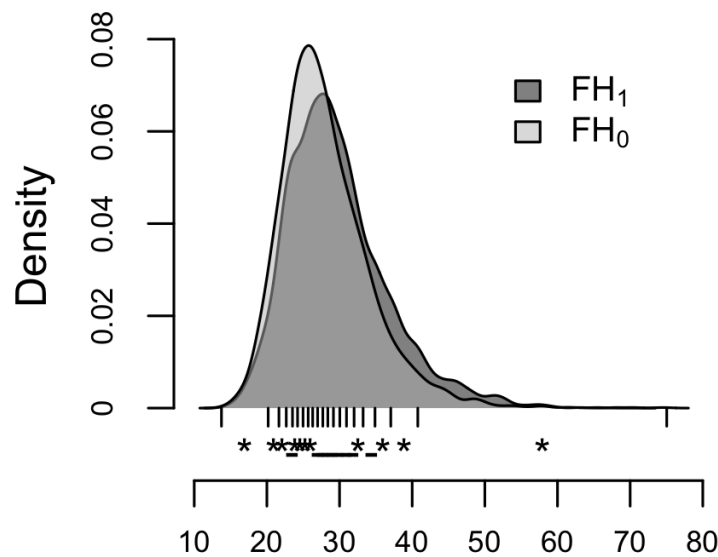
**Fig 3:** A) Adjusted BMI density in  $FH_1$  by quantile (grey bars) and kernel-smoothed (black line) with fits to a three component normal mixture distribution. B) Estimated contributions in  $FH_1$  of the components of the mixture distribution to the prevalence (mixture coefficients,  $\lambda$ ) and variance of adjusted BMI.

**Fig 4:** Effects of diabetes family history ( $FH_{0/1}$ ) on linear secular trends in age-, gender- and race/ethnicity-adjusted BMI mean  $\pm$  se (A) and standard deviation  $\pm$  se (B). Parameter estimates with 95% CI were obtained in ANCOVA models by stratified bootstrap resampling of all non-diabetic individuals (see Methods). Dotted lines enclose 95% CI on fitted values at each point;  $\beta$  = regression slope vs. time ( $kg/m^2$  per year);  $\Delta\beta = \beta_{FH1} - \beta_{FH0}$  (95%CI).

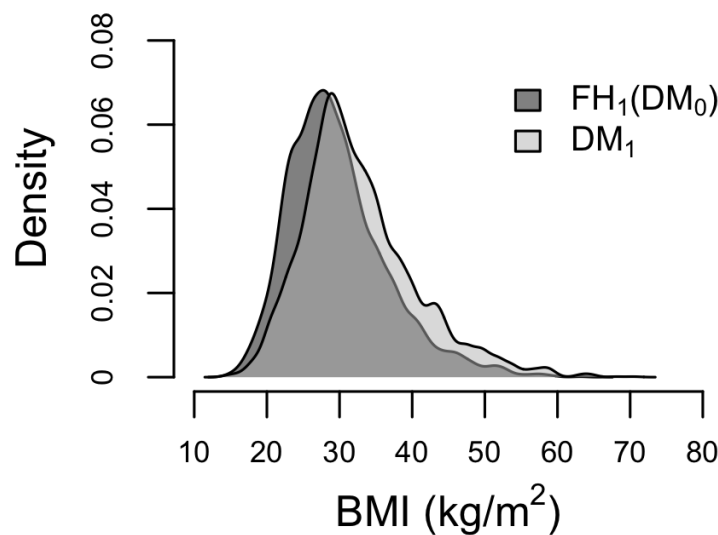
**A**

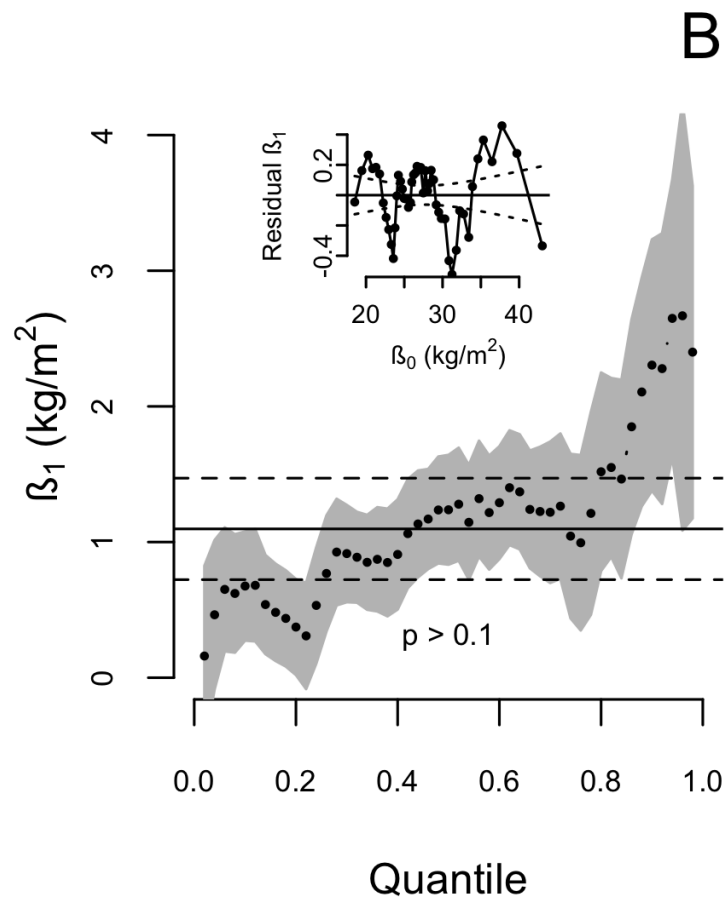
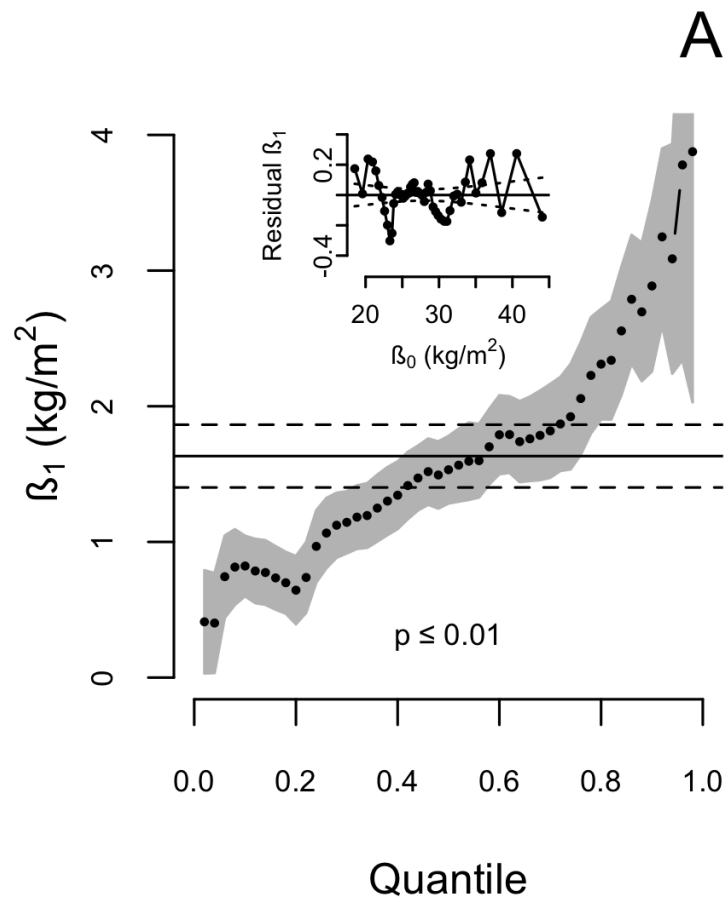


**B**

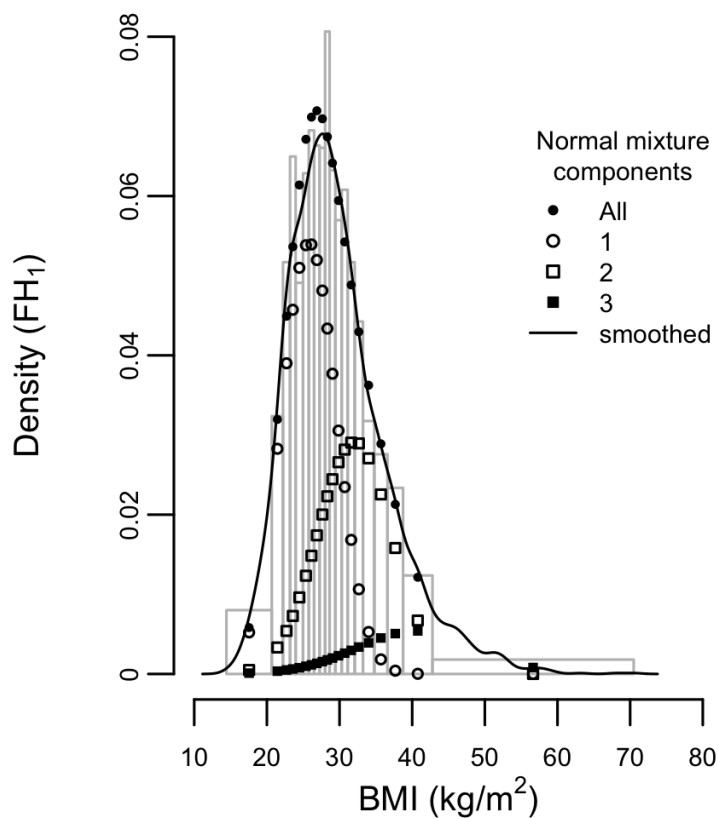


**C**

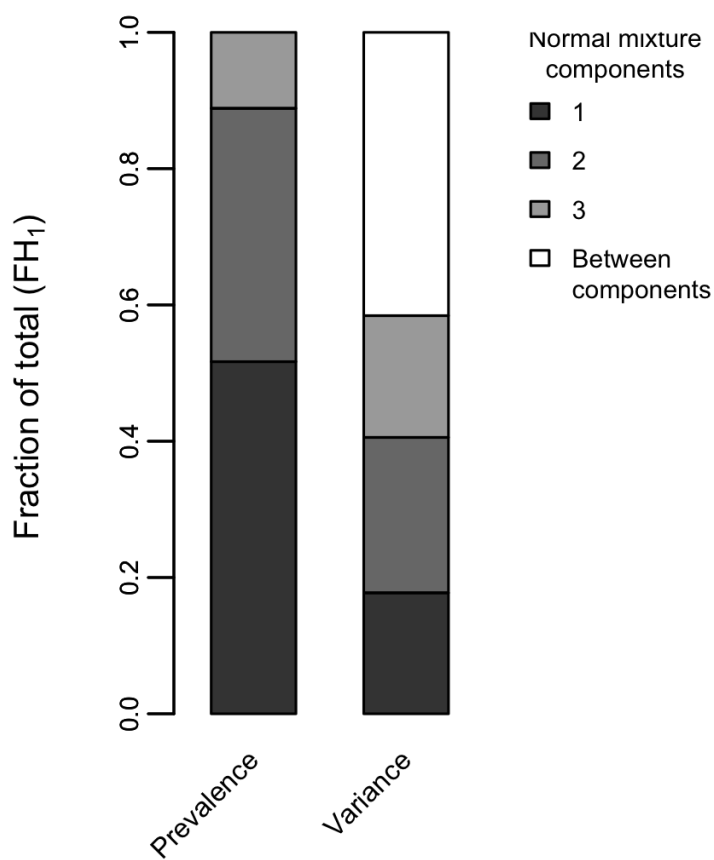




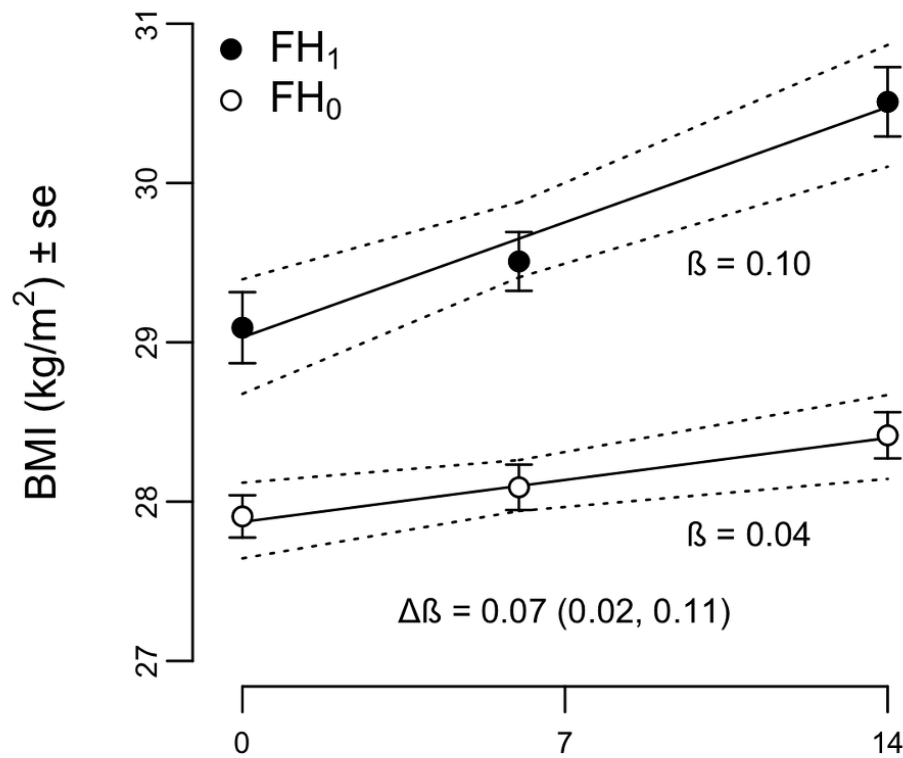
A



B



**A**



**B**

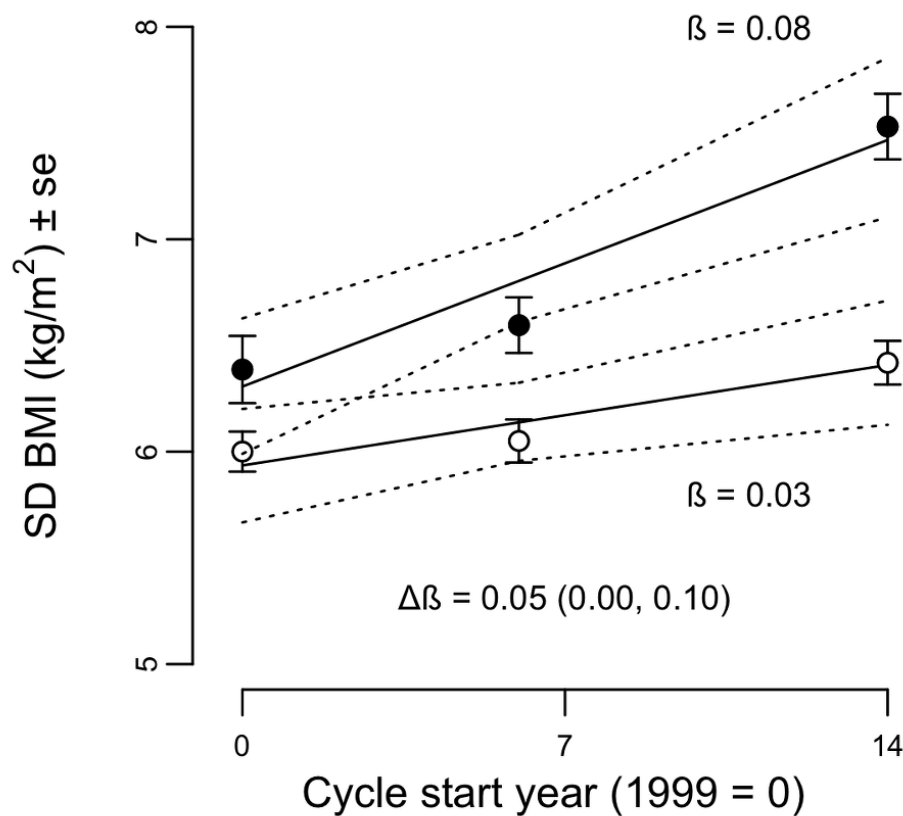


**Table 1: Participants by diabetes status (DM<sub>0</sub>/DM<sub>1</sub>)**

		NHANES cycle				
		All cycles	1999-2000	2005-2006	2013-2014	p <sup>†</sup>
DM <sub>0</sub>						
n		9102	2865	3076	3161	-
Gender (F%)		53	55	54	52	0.06
Race/Ethnicity (%)						
(MA/OH/NHW/NHB) <sup>‡</sup>		23/8/46/ 23	30/7/44/20	24/4/49/24	16/11/48/25	7.8 x 10 <sup>-56</sup>
Age (yr):	Mean	40.5	40.7	39.4	41.5	4.5 x 10 <sup>-9</sup>
	SD	13.2	13.2	13	13.2	0.63
BMI (kg/m <sup>2</sup> )*: Mean		28.7	28.3	28.6	29.2	4.6 x 10 <sup>-9</sup>
	SD	6.6	6.3	6.4	7.1	1.2 x 10 <sup>-11</sup>
Diabetes Family History (Y%)		36	29	42	38	4.1 x 10 <sup>-25</sup>
Current smoking						
(%, Y/N/missing)		25/20/55				-
DM <sub>1</sub>						
n (%)		793 (8.0)	211 (6.9)	252 (7.6)	330 (9.5)	0.0003
Age at Diagnosis (yr)		43.6	44.3	42.9	43.6	0.47

† Cycle effects (p) by ANOVA (age), ANCOVA (BMI), Bartlett's test (SD's) and Chi-squared test for categorical variables.

‡ MA = Mexican American, OH = Other Hispanic, NHW = Non-Hispanic White, NHB = Non-Hispanic Black

\* Adjusted for age, gender and race/ethnicity in a linear model (see Table S1).

**Table 2: Three-component normal mixture distribution fits to adjusted BMI by FH and DM status<sup>¥</sup>**

	Component	DM <sub>0</sub>		DM <sub>1</sub>
		FH <sub>0</sub>	FH <sub>1</sub>	
mean	1	*	25.8±1.0	*
	2	*	32.1±1.8	*
	3	*	40.6±2.5	*
sd	1	3.8	3.8±0.9	3.7
	2	5.7	5.1±1.2	4.5
	3	10	8.2±0.8	8.4
λ	1	0.67	0.52±0.16	0.28
	2	0.29	0.37±0.15	0.47
	3	0.04	0.11±0.06	0.25
q	-	0.18	0.30±0.10 (0.37) <sup>§</sup>	0.49

<sup>¥</sup> ± bootstrap standard error for FH<sub>1</sub> only

\* Means in FH<sub>0</sub> and DM<sub>1</sub> constrained to fitted values in FH<sub>1</sub>

<sup>†</sup> Calculated risk allele frequency in an additive Mendelian model of large effects

<sup>§</sup> Predicted from DM<sub>1</sub> mating randomly into the full sample.



